

J6.1 THE EFFECTS OF ENVIRONMENTAL VARIABILITY AND EXPERIMENTAL ERROR IN PARAMETERIZING AIR-SEA GAS FLUXES

William E. Asher*
University of Washington, Seattle, Washington

1. INTRODUCTION

Advances in techniques for measuring air-sea fluxes have resulted in several new oceanic data sets of oceanic gas fluxes. In addition, novel experimental methodologies and detailed microphysical process studies have provided new information concerning the fundamental mechanisms controlling air-water gas exchange. These field and laboratory data have been used in developing and testing air-sea gas exchange dependencies and have allowed commonly used conceptual models to be tested. However, even with the advances in the understanding of the process and the additional experimental capabilities, variability in both laboratory and field data as a function of a particular variable characterizing the major forcing functions (e.g., wind stress) has made development of a robust method for parameterizing the gas transfer velocity difficult.

In general, the air-sea flux of a sparingly soluble non-reactive gas at low to moderate wind speeds can be written as the product of a kinetic term, the air-sea gas transfer velocity k_L ($\mu\text{m s}^{-1}$), and a thermodynamic driving force defined in terms of the disequilibrium in chemical potential of the gas between the ocean and the atmosphere. This driving force is commonly expressed in terms of the air-water partial pressure difference, ΔP (kPa) assuming that most gases of interest will behave ideally so that the fugacity in each phase is equal to their partial pressure in that phase. Although there is some evidence that errors in ΔP can affect the measurement of k_L (Jacobs et al., 2002), this is by no means conclusive and this discussion will focus on the kinetic term k_L .

It is well understood that in the absence of bubbles k_L depends on both the molecular diffusivity, D ($\text{m}^2 \text{s}^{-1}$), of the gas in the aqueous phase and on the water-side turbulence very close to the free surface (Davies, 1972). However, the details of these dependencies as they relate to the particulars of gas transfer at the ocean surface are not well

known and still subject to considerable debate. For example, it is clear that the presence of naturally occurring surface active material (which will be referred to here as “surfactants” for short) can inhibit air-water gas transfer (Frew et al., 1990). However, it is less clear that field measurements of k_L can be easily partitioned into those made under surfactant-impacted conditions and those made under so-called clean conditions. Even more uncertain is how to best parameterize the role of turbulence in influencing the magnitude of k_L .

Under most conditions, the wind stress plays a dominant role in providing the turbulence kinetic energy involved in promoting gas exchange. Therefore, wind speed has long been used to parameterize k_L . Figure 1 shows k_L measured in the ocean using the purposeful dual-tracer method (Wanninkhof et al., 1993) plotted as a function of average wind speed. (The data in the figure were compiled from Wanninkhof et al. (1993), Wanninkhof et al. (1997), Jacobs et al. (1999), Nightingale et al. (2000b), Nightingale et al. (2000a) and Wanninkhof et al. (2004) and have all been scaled to a common diffusivity equal to carbon dioxide in seawater at 293.15 K, defined here in terms of the Schmidt number (660), assuming that k_L is proportional to $D^{1/2}$). When the values for the scaled transfer velocity, k_{660} , at a particular wind speed are compared, the data is considerably scattered. It can be argued that the overall dependence follows either a power law (or polynomial) dependence or a segmented linear dependence with wind speed. Unfortunately, there is too much scatter in the data to allow the data to provide a definitive selection between any of the available gas exchange parameterizations.

Figure 1 typifies the problem in attempting to develop a method for accurately estimating k_L from an easily measured environmental parameter. The data in the figure represent measurements of the highest quality, collected by meticulous and careful groups. Because of this, it is assumed that much of the scatter in the data represents variability in the transfer velocity imposed by variability in the environmental conditions. This could occur if, for example, the levels of aqueous-phase turbulence generated at a particular wind speed depend on factors other than the wind speed itself. This explanation seems logical on an intuitive level, but

*Corresponding author address: William E. Asher, Applied Physics Laboratory, Univ. of Washington, 1013 NE 40th Street, Seattle, WA 98105; e-mail: asher@apl.washington.edu

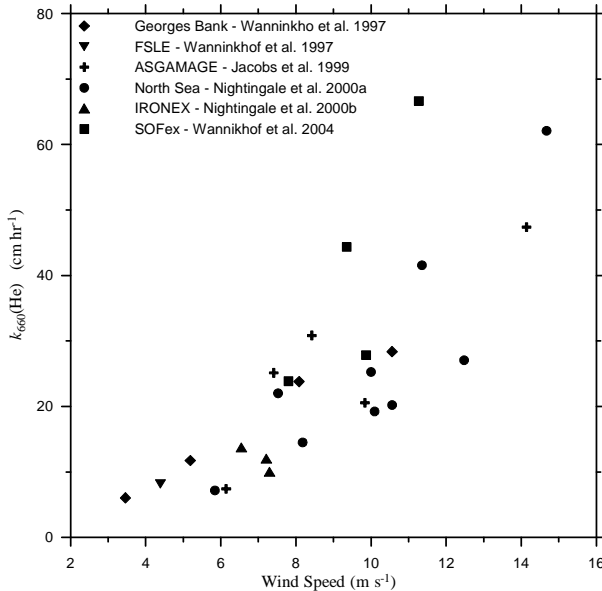


Figure 1: Available oceanic measurements of the air-sea gas transfer velocity made using the purposeful dual-tracer method normalized to a common Schmidt number of 660, $k_{660}(\text{He})$, plotted as a function of wind speed. The data key is shown on the figure.

the fundamental measurements of turbulence necessary to support it are not available. So it could be that the scatter in Figure 1 could simply represent experimental uncertainty rather than environmental variability.

The purpose of this paper is to explore whether it is possible to explain the scatter in various measurements of the transfer velocity simply in terms of the uncertainty in measuring the underlying parameters. This will be done using the dual-tracer data shown in Figure 1 and using gas transfer data collected in the Air-Sea Interaction Research Facility (ASIRF) at NASA Wallops Flight Facility.

2. THEORY

In the case where a non-reactive gaseous tracer is injected into a known volume of water, the change in concentration with respect to time due to the water-to-air gas flux can be written as

$$\frac{dC_B}{dt} = \frac{k_L A}{V} (K_H P_A - C_B) \quad (1)$$

where C_B is the bulk-phase concentration of the tracer gas (mol m^{-3}), A is the surface area of the water through which gas exchange occurs (m^2), V is the total water volume (m^3), K_H is the aqueous-phase

solubility of the gas ($\text{mol m}^{-3} \text{kPa}^{-1}$), and P_A is the partial pressure of the gas in the air phase (kPa). Integration of Eq. 1 shows that k_L can be written as

$$k_L = \frac{V}{A \Delta t} \ln \left(\frac{C_s - C_0}{C_s - C_B} \right) \quad (2)$$

where Δt is the time difference and C_0 is the concentration of the tracer gas at time $t=0$. From Eq. 2, a plot of the quantity $-\ln((C_s - C_0)/(C_s - C_B))$ versus time will result in a straight line with slope equal to $k_L A/V$.

A similar relation exists for the analysis of purposeful dual-tracer data collected during oceanic air-sea gas exchange measurements. In these experiments, the two volatile tracer gases sulfur hexafluoride (SF_6) and helium-3 (${}^3\text{He}$) are injected into the surface mixed layer. Their concentrations are then measured as a function of time and the transfer velocity of ${}^3\text{He}$, $k_L({}^3\text{He})$, can be estimated from the change in the concentration ratio of the two tracers. This relation has the form

$$k_L({}^3\text{He}) = \frac{h}{\Delta t} \frac{\Delta \left[\ln \left(\frac{[{}^3\text{He}]}{[\text{SF}_6]} \right) \right]}{\left\{ 1 - \left[\frac{\text{Sc}({}^3\text{He})}{\text{Sc}(\text{SF}_6)} \right]^{1/2} \right\}} \quad (3)$$

where h is the mixed layer depth, Δt is the time interval over which the change in concentrations are measured, $[{}^3\text{He}]$ and $[\text{SF}_6]$ are the concentrations of ${}^3\text{He}$ and SF_6 , respectively, and $\text{Sc}({}^3\text{He})$ and $\text{Sc}(\text{SF}_6)$ are the Schmidt numbers of ${}^3\text{He}$ and SF_6 , respectively.

Applying either Eq. 2 or Eq. 3 is straightforward and their theoretical bases are not in dispute. However, because of the logarithmic relationship involving the concentrations and the fact that the change in concentration with respect to time can be relatively small, both equations are sensitive to measurement uncertainty.

In laboratory experiments, it is common to simultaneously measure k_L for several gases. From these data, it is possible to estimate the dependence of k_L on molecular diffusivity. In general, conceptual models for air-water gas transfer assume that this dependence can be written as

$$k_L = a \left(\frac{v}{D} \right)^{-n} f(Q, L) \quad (4)$$

where a and n are constants, ν is the kinematic viscosity of water, and $f(Q, L)$ symbolizes the as yet unspecified dependence of k_L on the turbulence velocity and length scales. The ratio ν/D is the Schmidt number, Sc , and it will be used from this point in place of D . Depending on the conceptual model, n can range from 1/2 to 2/3 with the lower value usually associated with gas exchange through a clean water surface and higher values associated with transfer through surfactant influenced surfaces. Therefore, the dependence of k_L on Sc provides very useful information on the transfer process and it is highly desirable to be able to estimate n from experimental data.

Using Eq. 4, it can be shown that if the k_L values for two gases with different Sc numbers are known, n is equal to

$$n = \frac{\ln[k_L(1)/k_L(2)]}{\ln[Sc(2)/Sc(1)]} \quad (5)$$

where the (1) and (2) refer to the parameter for the two respective gases. As is the case for calculating k_L itself, Eq. 5 is also sensitive to measurement errors because Sc for most gases does not vary by a large amount.

3. LABORATORY STUDIES

The Flux Exchange Dynamics Study (FEDS) was conducted at the ASIRF wind-wave tunnel at NASA-WFF in 1998. During the study, k_L was measured for SF_6 and helium (He) using gas chromatography to determine aqueous-phase gas concentrations. Method precision for gas concentrations was found to be $\pm 3\%$ for SF_6 and $\pm 7\%$ for He. Figure 2 shows transfer velocities for SF_6 normalized to $Sc=600$ assuming $n=1/2$, $k_{600}(SF_6)$, measured during FEDS plotted as a function of wind speed. Figure 3 shows transfer velocities measured during FEDS for He normalized to $Sc=600$, $k_{600}(He)$, also plotted versus wind speed. Sc values for SF_6 were taken from King and Saltzman (1995) and for He from Wanninkhof (1992).

In similarity with the field measurements of k_L , there is some scatter in the measured values of the transfer velocity when plotted as a function of wind speed. In order to test whether this scatter could be due to experimental uncertainty, a Monte Carlo-type simulation was performed using the known experimental uncertainties to estimate the variability in k_L that would be expected given the uncertainties in the concentrations.

The first step in this procedure was to use the

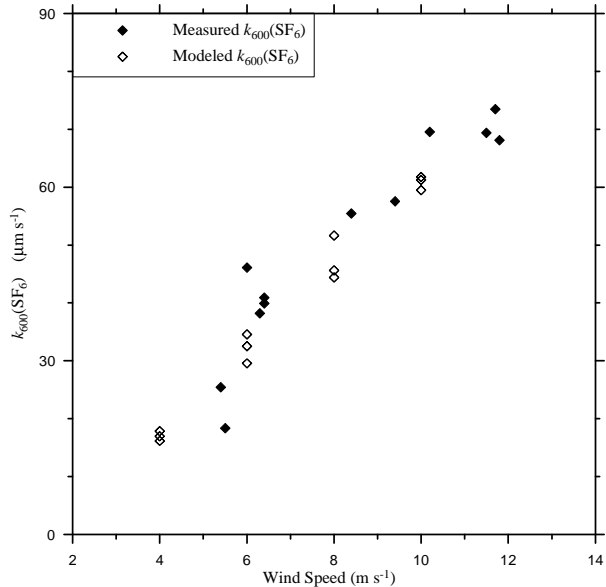


Figure 2: The air-water gas transfer velocity for SF_6 normalized to $Sc=600$, $k_{600}(SF_6)$, measured during FEDS plotted as a function of wind speed. Also shown are values for $k_{600}(SF_6)$ produced by the Monte Carlo model described in Section 3. The data key is shown on the

experimental data in Figures 2 and 3 to produce a linear relation for estimating k_L from wind speed in the ASIRF wind-wave tunnel. This showed that k_L could be written as

$$k_{600}(Sc) = \left(\frac{600}{Sc} \right)^{1/2} (7.7 \times 10^{-6} U - 1.5 \times 10^{-5}) \quad (6)$$

for k_L in $\mu\text{m s}^{-1}$ and wind speed U in m s^{-1} . Then, Eq. 2 was rewritten in the form

$$C_B = C_S - (C_S - C_0) \exp\left(-\frac{Ak_L t}{V}\right) \quad (7)$$

so that gas concentrations could be predicted as a function of t . Concentrations were predicted at five times with time steps on the order of 3000 s so that the number of modeled concentrations and their time steps were equal to those used in the actual data. Then, the predicted concentrations were modified by adding or subtracting a random amount determined by the measurement error for that particular gas. Three separate sets of concentrations were produced for each gas at $U=4 \text{ m s}^{-1}$, 6 m s^{-1} , 8 m s^{-1} , and 10 m s^{-1} . These modified concentrations were then used in Eq. 2 to calculate $k_{600}(SF_6)$ and $k_{600}(He)$ the resulting values are shown in Figures 2 and 3, respectively.

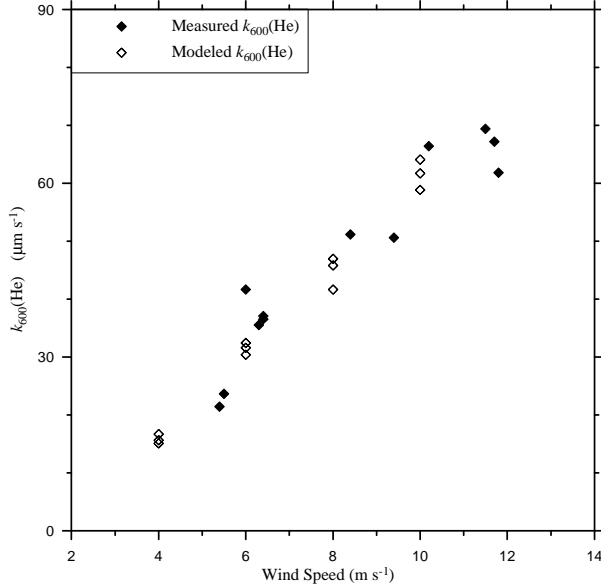


Figure 3: The air-water gas transfer velocity for SF_6 normalized to $\text{Sc}=660$, $k_{660}(\text{SF}_6)$, measured during FEDS plotted as a function of wind speed. Also shown are values for $k_{660}(\text{SF}_6)$ produced by the Monte Carlo model described in Section 3. The data key is shown on the figure.

The values of the modeled transfer velocities at a given wind speed show a scatter that is similar to what was measured experimentally. This suggests that the variability in the data is due to the measurement precision and not differences in the environmental conditions from run to run.

The modeled concentrations can also be used to study the variability in values of n deduced from measurements of k_L . Figure 4 shows n calculated using Eq. 5 and $k_L(\text{SF}_6)$ and $k_L(\text{He})$ measured in the ASIRF during FEDS plotted versus wind speed. Also shown in Figure 4 are values of n calculated using Eq. 5 with the modeled transfer velocities shown in Figures 2 and 3. As expected for a clean surface, the data are clustered around $\frac{1}{2}$, although there are particular data points that lie significantly above and below a value of 0.5. As was seen in the transfer velocities themselves, the predicted variability from the Monte Carlo simulations is of the same order as the variability in the experimental data. This suggests that the variability observed in Figure 4 is not due to environmental variability and merely reflects the sensitivity of n to experimental uncertainty.

In the above analysis of the variability in n , it was assumed that n was equal to $\frac{1}{2}$ and constant as a function of wind speed. However, laboratory data exists suggesting that n is a function of U , decreasing from $\frac{2}{3}$ to $\frac{1}{2}$ as U increases (Jähne et

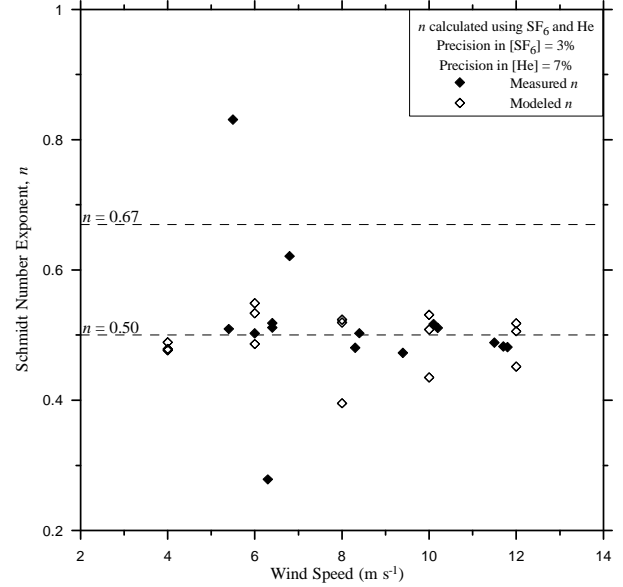


Figure 4: The Schmidt number exponent, n , calculated using Eq. 5 and gas transfer velocity data for the gas pair SF_6 and He . The data key is shown on the figure.

al., 1984; Zappa et al., 2001). Because of this, it is desirable to be able to use the gas transfer measurements to determine the dependence of n on wind speed.

The Monte Carlo method described above was used to assess how measurement errors might affect determining the functionality of n with respect to U . First, it was assumed that n was given by

$$n = 0.67 : \quad U < 2 \text{ m s}^{-1}$$

$$n = 0.5 + 0.17e^{-\left(\frac{U-2}{2}\right)} : \quad U \geq 2 \text{ m s}^{-1} \quad (8)$$

and then k_L values were calculated for the gases methane, CH_4 , SF_6 , and He using Eq. 6 using n calculated using Eq. 8 in place of the exponent $\frac{1}{2}$. Sc values for CH_4 were taken from Wanninkhof (1992). Five wind speeds were used, from a minimum of 4 m s^{-1} to a maximum of 12 m s^{-1} in increments of 2 m s^{-1} . As before, three separate concentration time series that included a $\pm 3\%$ random error in each value were generated for each gas. Then, k_L was calculated using each concentration time series. An estimate of n could then be derived using the gas pairs CH_4/SF_6 , CH_4/He , and SF_6/He . Figure 4 shows the results of this procedure along with the actual value of n used to produce the gas concentrations.

The top panel in Figure 5 shows the values for n calculated using CH_4/SF_6 . Because the change in Sc value for these two gases is relatively small (e.g.,

$\text{Sc}(\text{CH}_4) = 616$ @ 293.15 K, $\text{Sc}(\text{SF}_6) = 948$ @ 293.15 K), the effect of measurement error is large and there is no clear dependence of n on wind speed. The situation improves for both gas pairs involving He, mainly because $\text{Sc}(\text{He}) = 149$ under these conditions. However, the variability in the calculated values for n are still too large for accurately resolving the assumed dependence of n on wind speed.

4. FIELD MEASUREMENTS

The Monte Carlo method described in the previous section can also be applied to the purposeful dual-tracer method (PDTM). However, in the case of PDTM data analysis, in addition to the measurement uncertainties in the gas concentrations, the uncertainty in the mixed layer depth, h , must also be taken into account. As discussed by Wanninkhof et al. (2004), the analysis of PDTM data proceeds by analyzing discrete segments of the times series for the two gases over intervals where the wind speed was relatively constant. Rather than address the effect of averaging wind speed, which has been discussed in some detail elsewhere (Wanninkhof et al., 2004), here the effect of measurement variability under steady winds will be studied.

Here, it was assumed that the concentrations of both SF_6 and ^3He could be measured in the ocean with a precision of $\pm 2\%$ (R. Wanninkhof, NOAA Atlantic Oceanographic and Meteorological Laboratory, Miami Florida, personal communication). The uncertainty in h is more problematic, and it was assumed to be $\pm 20\%$ (D. Ho, Lamont Doherty Earth Observatory, Palisades New York, personal communication).

The Monte Carlo simulations were carried out by calculating the transfer velocities of SF_6 and He as a function of wind speed using the U^2 power law dependence proposed by Wanninkhof (1992). Eq. 7 was used with the calculated k_L values assuming $h = 50$ m and that $h = V/A$ to generate a concentration time series for SF_6 and He. Two concentrations were taken from the time series with a Δt in the range of 1-2 days. These concentrations were used in Eq. 3 to calculate $k_L(^3\text{He})$ at wind speeds of 4 m s^{-1} , 8 m s^{-1} , 12 m s^{-1} and 16 m s^{-1} . Figure 6 shows the data from Figure 1 along with the transfer velocities calculated from the Monte Carlo procedure. With the exception of the PDTM results from SOFex (Wanninkhof et al., 2004), the observed variability in the results is within the limits of the variability produced solely by the assumed measurement uncertainties. This suggests that environmental variability may not play as large a role as supposed.

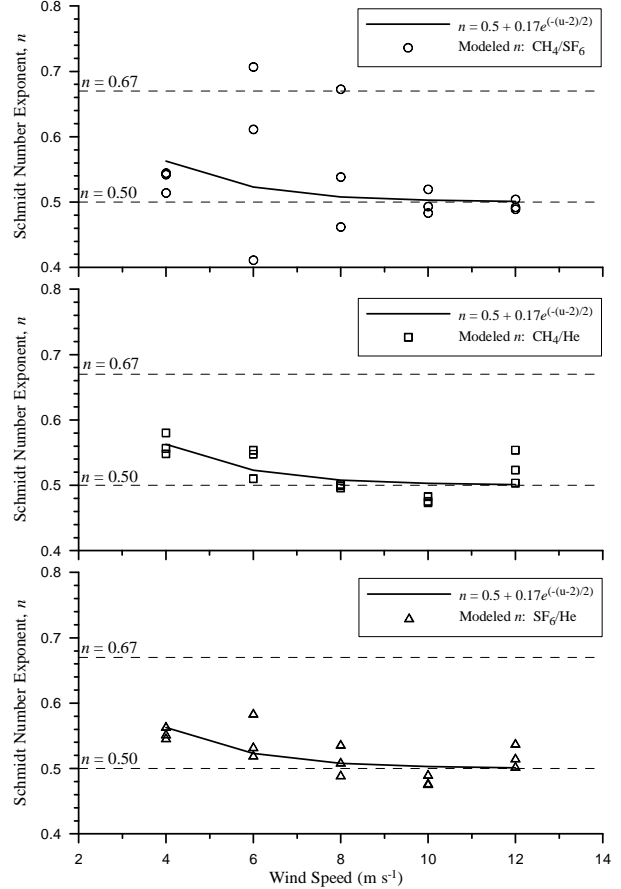


Figure 5 : Plots of the Sc exponent n as calculated using the Monte Carlo procedure described in the text plotted as a function of wind speed. The assumed dependence of n on wind speed used to generate the values of n is shown in each plot. The data key is shown on the figure.

5. CONCLUSIONS

The simple Monte Carlo model used here does not account for all sources of experimental variability in measuring air-water gas transfer velocities. However, it is instructive that using realistic values for the uncertainties in the concentration measurements and estimations of the mixed layer depth, much of the observed variability in the measured transfer velocities can be explained. This suggests that in both the field and laboratory there is less variability in the forcing mechanisms driving gas exchange than previously thought and that perhaps the overall pattern of the data in Figure 6 is somewhat close to the “true” functional dependence of k_L on wind speed. In turn, this is relatively good news for those who hope to develop a robust method for parameterizing gas transfer in terms of

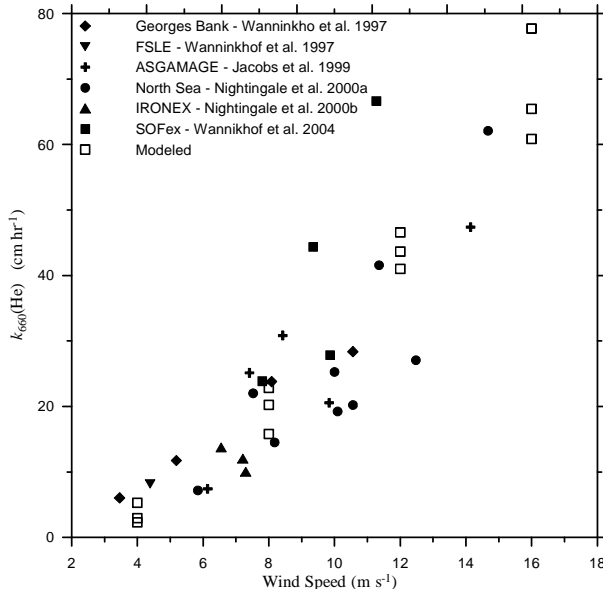


Figure 6: Air-sea gas transfer velocities of helium-3 normalized to $Sc=660$, $k_{660}(^3\text{He})$, measured using the purposeful dual-tracer method (PDTM). Also shown are $k_{660}(^3\text{He})$ values produced by the Monte Carlo simulations described in Section 4. The data key is shown on the figure.

an easily measured environmental variable. However, it also points out the difficulty associated with making the measurements used to validate these parameterizations.

6. REFERENCES

Davies, J. T., 1972: *Turbulence Phenomena: An Introduction to the Eddy Transfer of Momentum, Mass, and Heat, Particularly at Interfaces*. Academic Press, 412 pp.

Frew, N. M., Goldman, J. C., Dennett, M. R., and Johnson, A. S., 1990: Impact of phytoplankton-generated surfactants on air-sea gas exchange. *J. Geophys. Res.*, **95C**, 3337-3352.

Jacobs, C., Kjeld, J. F., Nightingale, P., Upstill-Goddard, R., Larsen, S., and Oost, W., 2002: Possible errors in CO₂ air-sea transfer velocity from deliberate tracer releases and eddy covariance measurements due to near-surface concentration gradients. *J. Geophys. Res.-Oceans*, **107**.

Jacobs, C. M. J., Kohsieck, W., and Oost, W. A., 1999: Air-sea fluxes and transfer velocity of CO₂ over the North Sea: results from ASGAMAGE. *Tellus Series B-Chemical and Physical Meteorology*, **51**, 629-641.

Jähne, B., Huber, W., Dutzi, A., Wais, T., and Ilmberger, J., 1984: Wind/wave tunnel experiments on the Schmidt number and wave field dependence of air-water gas exchange. *Gas Transfer at Water Surfaces*, W. Brutsaert and G. H. Jirka, Eds., Reidel, 303-310.

King, D. B. and Saltzman, E. S., 1995: Measurement of the diffusion coefficient of sulfur hexafluoride in water. *J. Geophys. Res.*, **100**, 7083-7088.

Nightingale, P. D., Liss, P. S., and Schlosser, P., 2000a: Measurements of air-sea gas transfer during an open ocean algal bloom. *Geophys. Res. Lett.*, **27**, 2117-2120.

Nightingale, P. D., Malin, G., Law, C. S., Watson, A. J., Liss, P. S., Liddicoat, M. I., Boutin, J., and Upstill-Goddard, R. C., 2000b: In situ evaluation of air-sea gas exchange parameterizations using novel conservative and volatile tracers. *Global Biogeochem. Cycles*, **14**, 373-387.

Wanninkhof, R., 1992: Relationship between wind speed and gas exchange over the ocean. *J. Geophys. Res.*, **97**, 7373-7382.

Wanninkhof, R., Asher, W. E., Weppernig, R., Chen, H., Schlosser, P., Langdon, C., and Sambrotto, R., 1993: Gas transfer experiment on Georges Bank using two volatile deliberate tracers. *J. Geophys. Res.*, **98**, 20,237-20,248.

Wanninkhof, R., Hitchcock, G., Wiseman, W., Ortner, P., Asher, W., Ho, D., Schlosser, P., Dickson, M.-L., Anderson, M., Masserini, R., Fanning, K., and Zhang, J.-Z., 1997: Gas exchange, dispersion, and biological productivity on the west Florida shelf: Results from a Lagrangian tracer study. *Geophys. Res. Lett.*, **24**, 1767-1770.

Wanninkhof, R., Sullivan, K. F., and Top, Z., 2004: Air-sea gas transfer in the Southern Ocean. *J. Geophys. Res.-Oceans*, **109**.

Zappa, C. J., Asher, W. E., and Jessup, A. T., 2001: Microscale wave breaking and air-water gas transfer. *J. Geophys. Res.*, **106**, 9385-9392.